Journal of Photochemistry and Photobiology A: Chemistry 223 (2011) 165–171

Contents lists available at SciVerse ScienceDirect

Journal of Photochemistry and Photobiology A: Chemistry

journal homepage: www.elsevier.com/locate/jphotochem

Atmospheric chemistry of 2-ethyl hexanal: Photochemistry and oxidation in the presence of NO_2

Juan C. Fraire, Gustavo A. Argüello, Fabio E. Malanca*

INFIQC (CONICET), Departamento de Fisicoquímica, Facultad de Ciencias Químicas, Universidad Nacional de Córdoba, Ciudad Universitaria, 5000 Córdoba, Argentina

ARTICLE INFO

Article history:
Received 24 May 2011
Received in revised form 12 August 2011
Accepted 18 August 2011
Available online 27 August 2011

Keywords:
2-Ethyl hexanal
Atmospheric oxidation
Photochemistry
Peroxy nitrates

ABSTRACT

The photolysis and oxidation mechanism of 2-ethyl hexanal ($C_4H_9CH(C_2H_5)C(O)H$—2-Ethal) have been investigated. The UV absorption cross sections were recorded over the range 200–350 nm at 298 K. The quantum yield for photolysis at 254 nm was determined to be 0.51 ± 0.09. Photolysis of 2-Ethal occurs by two primary paths: a concerted elimination path and a radical formation path, the latter being the main path. CO, heptane, 3-heptanol, and 3-heptanone were identified as the main products.

The rate constant for the reaction with Cl atoms was determined using the relative rate technique with isopentane and cyclohexane as reference gases. The average rate constant obtained was $k = (2.8 \pm 0.9) \times 10^{-10}$ cm^3 molecule^{-1} s^{-1}. The most important path in the oxidation mechanism was the acyl radical forming channel, which was corroborated by the analysis of the products formed via photolysis in the presence of NO_2. Those products were CO_2, CO, peroxyacetyl nitrate, peroxypropionyl nitrate, and ethyl nitrate.

1. Introduction

Aldehydes are important atmospheric constituents and are emitted by a variety of natural and anthropogenic sources, such as incomplete fossil fuel combustion, vegetation, biomass burning, and atmospheric oxidation of volatile organic compounds (VOCs). Aldehydes are important precursors of peroxyacyl nitrates ($RC(O)OONO_2$) [1], which play an important role in sequestering NO_x. The main atmospheric degradation paths of aldehydes are photolysis and reaction with OH with minor contributions from reactions with NO_3 and O_3 [2,3].

The available kinetic and mechanistic data show that the main reaction pathway of OH radicals corresponds to the H-atom abstraction of the aldehydic group (acyl forming channel), and has values of 80–90% for acetaldehyde, propionaldehyde and benzaldehyde [4,5]. It should be noted that in many laboratory measurements the oxidation reaction is initiated by photolysis of chlorine with black lamps (wavelengths longer than 360 nm) since it provides similar results. Studies carried out by Le Crane et al. indicate that the acyl-forming channel accounts for 80–90% of the reaction of Cl atoms with small aldehydes [6]. In the presence of O_2 and NO_2, the acyl radicals ($RC(O)$) form peroxyacyl nitrates ($RC(O)–OONO_2$), which are reservoir species. The stability of these compounds depends on the structure of the peroxy radical from which they are formed, with thermal lifetimes ranging from hours to several days [7]. Since stability increases at low temperatures, these compounds are stable in the middle troposphere and in the tropopause, allowing transport to remote locations where they can release ROO and NO_2 radicals, contributing to the formation of tropospheric ozone [8–10].

Photodissociation of aldehydes has been studied by several authors. Recently, Wirtz [11] and Moortgat et al. [12,13] have carried out studies in the European Photo-reactor (EUPHORE) determining the quantum yields and the possible photolytic pathways of several aldehydes including pentanal, hexanal, butyraldehyde, 2-methyl butyraldehyde, and 3-methyl butyraldehyde. The quantum yield values are commonly less than unity. For α-branched compounds, however, it is about twice the value for the linear analogue. The primary photodissociation pathways can generate both molecular species and radicals, depending on the structure of the aldehyde [11].

We present in this work a kinetic and photochemical study of 2-ethyl hexanal (2-Ethal, $C_4H_9CH(C_2H_5)C(O)H$), a widely used solvent [14] having a vapor pressure of 2.6 mbar at 298 K, which is also the main product of the atmospheric degradation of 2-ethyl hexanol, another common solvent [15,16]. Previous studies of 2-Ethal oxidation in the liquid phase [17] and the gas-phase [18] giving 2-ethyl hexanoico acid highlight its use as a large scale reagent.

2. Experimental

2.1. Chemicals

Commercially available samples of 2-Ethal (Aldrich), isopentane (Cicarelli), cyclohexane (Dorwil), perfluoroacetic anhydride

* Corresponding author. Tel.: +54 351 433 4169; fax: +54 351 433 4188.
E-mail address: fmalanca@fcq.unc.edu.ar (F.E. Malanca).

1010-6030/$ – see front matter © 2011 Elsevier B.V. All rights reserved.
doi:10.1016/j.jphotochem.2011.08.014

(Aldrich), NO and O_2 (AGA) were used. Oxygen was condensed whilst flowing at atmospheric pressure through a trap immersed in liquid nitrogen. It was then pumped under vacuum several times and transferred to a glass bulb whilst the trap was still immersed in liquid nitrogen. NO_2 was prepared by adding O_2 to NO and further purified after reaction. Cl_2 was synthesized by direct reaction between HCl and $KMnO_4$ in a nitrogen flux, collected into liquid air, and further distilled.

2.2. Methods

The manipulation of reactants and products was performed using a conventional vacuum gas system. The change in reactant concentration with time and the identification of products were monitored using a Bruker IFS-66v Fourier Transform Infrared Spectrophotometer (FTIR).

2.2.1. Rate constant of chlorine atoms with 2-Ethal

The set-up used for the relative rate measurements consists of a 22.0 cm optical path glass cylinder reaction cell with silicon windows, located in the optical path of the FTIR. Typical experiments used mixtures of 2-Ethal (1.5 mbar), reference gas (1.5 mbar), Cl_2 (0.5 mbar), and O_2 (900 mbar) at 298 K, using a black lamp that provides wavelengths longer than 360 nm. The temporal variation in reactants was followed collecting infrared spectra with a resolution of 2 cm^{-1}.

Relative rate constant experiments were conducted using either isopentane (i-C_5H_{12}) or cyclohexane (C_6H_{12}) as the reference gas (RG):

$$\text{2-Ethal} + \text{Cl} \rightarrow \text{Products} \quad (1)$$

$$\text{RG} + \text{Cl} \rightarrow \text{Products} \quad (2)$$

Assuming that the aldehyde and the reference compound react only with Cl, it can be shown that:

$$\ln\left(\frac{[\text{2-Ethal}]_0}{[\text{2-Ethal}]_t}\right) = \frac{k_1}{k_2}\ln\left(\frac{[\text{RG}]_0}{[\text{RG}]_t}\right)$$

where $[\text{2-Ethal}]_0$, $[\text{2-Ethal}]_t$, $[\text{RG}]_0$, and $[\text{RG}]_t$ indicate substrate and reference concentrations before and at time t of irradiation, respectively. A Ln–Ln plot of the former expression should be linear, with a slope (k_1/k_2) from which the rate constant of interest could be obtained.

In relative rate experiments it is important to check for unwanted loss of reactant and reference via direct photolysis, dark chemistry, or heterogeneous reactions. There was no observable loss of the reference gas neither in the dark nor upon irradiation of the mixture, in the absence of Cl_2. However, a minimal loss (5% after 30 min) of 2-Ethal was observed and attributed to heterogeneous processes since 2-Ethal does not absorb the radiation from black lamps, as discussed below. When Cl_2 was added in the dark there was no further loss of 2-Ethal.

2.2.2. Photo-reactor experiments

The analysis of products was carried out in a photo-reactor consisting of a 12 L round glass flask surrounded by three black lamps, inside a wooden box whose internal walls were covered with aluminium foil to maximize the reflected light. The surface/volume ratio of this particular photo-reactor is by far smaller than that of the IR cell used to determine the rate constant, thus minimising the participation of heterogeneous processes.

A mixture containing 2-Ethal (2.5 mbar)/Cl_2 (1.0 mbar)/NO_2 (0.7 mbar)/O_2 (900 mbar) was introduced into the photo-reactor and photolyzed for 90 min. The resulting sample was expanded to a long path infrared gas cell (optical path 9.0 m), and an IR spectrum was collected.

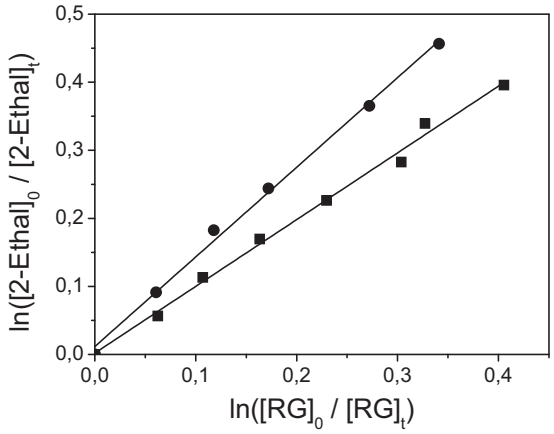

Fig. 1. Variation of 2-Ethal concentration as a function of the reference gas concentration. Different symbols represent separate experiments: isopentane (circle) and cyclohexane (square).

Since our aim is to produce peroxynitrates, the photolysis time was adjusted to avoid complete disappearance of NO_2. Short photolysis times produce a low yield overall; long photolysis times, in turn, lead to a low NO_2/NO ratio (NO formed by the slow photolysis of NO_2), which favors the formation of non-RNO_2 products. The optimum time chosen was 90 min.

2.2.3. Quantum yield (ϕ) measurements and photolysis experiments

UV absorption cross sections (σ) of 2-Ethal from 200 to 355 nm were determined using a standard UV gas cell (optical path 10 cm) located on the optical axis of a UV–vis spectrophotometer with a diode array detector. A calibration curve was obtained for pressures ranging between 0.5 and 2.0 mbar.

Photolyses at 254 nm (low pressure mercury lamp) were performed using a quartz cell (optical path 22 cm) with KBr windows that allowed simultaneous FTIR measurements.

Mixtures of 2-Ethal (1.5 mbar)/O_2 (900 mbar) were introduced into the cell and photolyzed for 35 min. A chemical actinometer (perfluoro acetic anhydride, APFA, $(CF_3C(O))_2O$, $\sigma_{254\,nm} = (2.28 \pm 0.03) \times 10^{-19}$ cm^2 $molecule^{-1}$, $\phi_{254\,nm} = (0.29 \pm 0.02)$) was employed [27]. All measurements were performed in the presence of O_2 to scavenge the radicals formed in the photolysis and ensure that they do not contribute to the disappearance of the aldehydes through secondary reactions.

In experiments where products had to be identified, the photolysis times were the same as those used in the photo-reactor experiments.

3. Results and discussion

3.1. Rate constant of chlorine atoms with 2-Ethal

Fig. 1 shows the 2-Ethal loss relative to isopentane (circles) and cyclohexane (squares). As mentioned before, the slope of the least-squares line provides the rate constant ratio k_1/k_2, from which the rate constant for 2-Ethal can be derived.

The rate constant ratio obtained using isopentane as reference, k_1/k_2 was 1.34 ± 0.09. The quoted uncertainty includes the standard deviation from the least-squares of the slope shown in Fig. 1 and also the uncertainty associated with the correction to account for heterogeneous loss of 2-Ethal. Assuming that the value reported by Anderson et al. for the rate constant between chlorine atoms and isopentane, $k_2 = (1.93 \pm 0.07) \times 10^{-10}$ cm^3 $molecule^{-1}$ s^{-1} [19] is the best available, the resulting value of k_1 is

Table 1
Rate constants for the reaction of aldehydes with chlorine atoms at 298 K.

Compound	Rate constant (10^{-10} cm^3 molecule^{-1} s^{-1})	Reference
Propionaldehyde	1.1 ± 0.1	[22]
n-Butyraldehyde	1.38 ± 0.18	
n-Pentanal	1.89 ± 0.24	
n-Hexanal	2.55 ± 0.21	
n-Heptanal	2.96 ± 0.56	
iso-Butyraldehyde	1.7 ± 0.3	[2]
tert-Butyraldehyde	1.6 ± 0.3	
2-Ethyl hexanal	2.8 ± 0.9	This work

$(2.6 \pm 0.3) \times 10^{-10}$ cm^3 molecule^{-1} s^{-1}. When cyclohexane was used as reference, the ratio k_1/k_2 was 1.0 ± 0.1. The same procedure described above for isopentane was used to deal with the error limits. From the value reported by Li et al. for the rate constant between chlorine atoms and cyclohexane, $k_2 = (2.9 \pm 0.3) \times 10^{-10}$ cm^3 molecule^{-1} s^{-1} [20], the resulting value of k_1 is $(2.9 \pm 0.7) \times 10^{-10}$ cm^3 molecule^{-1} s^{-1}.

Table 1 compares the mean value of k_1 obtained from the two different reference gases with the corresponding ones for other aldehydes. The comparison reveals that the rate constant determined in this work is consistent with the trend of increasing reactivity with increasing the size of aldehydes [2,20].

3.2. Oxidation mechanism in the presence of NO_2 at 298 K

Fig. 2 shows the spectrum of the products of the photooxidation mechanism in the presence of NO_2. The presence of hydrogen chloride, carbon dioxide, and carbon monoxide is clearly distinguishable. The spectrum also reveals the presence of characteristic bands for peroxynitrates, RC(O)OONO$_2$ (CO stretch, ν_1; ONO antisymmetric stretching, ν_2; and ONO scissoring, ν_3) and nitrates, RONO$_2$ (ONO antisymmetric stretching, ν_4 and ONO scissoring, ν_5).

Fig. 3 presents a sequence of spectra allowing the positive identification of the substances involved in the reaction. The upper trace shows the spectrum of pure 2-Ethal, and the following trace corresponds to the whole mixture after photolysis. The next trace is the result of subtracting features corresponding to nitrosyl chloride and nitric acid, identified in the figure by their characteristic bands (ClNO—1809 and 1789 cm^{-1}, HNO$_3$—1325 cm^{-1}). The presence of other known substance, namely peroxyacetyl nitrate—PAN (identified by its 1843, 1742, 1302, 1163 and 791 cm^{-1} bands), is evidenced by the third trace. The PAN spectrum is subtracted to yield the fourth trace, thus providing conclusive proof of the presence of peroxypropionyl nitrate (PPN), whose bands (1835, 1738, 1301, 1044 and 796 cm^{-1}) had been hidden by the features of PAN.

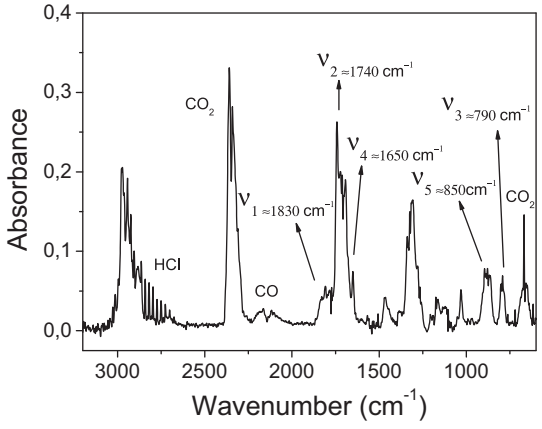

Fig. 2. Spectrum of 2-Ethal photooxidation products obtained in the presence of NO_2. Wavenumbers ν_{1-3} are typical of peroxynitrates and ν_{4-5} of nitrates.

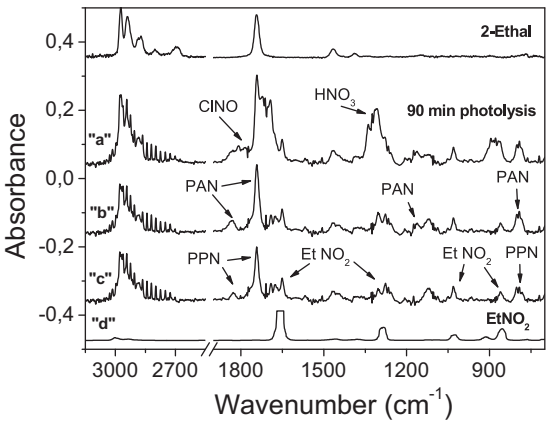

Fig. 3. Oxidation of 2-Ethal in the presence of NO_2. From top to bottom: 2-ethyl hexanal reference spectrum; reaction products obtained after 90 min of photolysis ("a" shows the presence of CO, CO_2 and HCl); "b" = "a"–HNO_3–ClNO; "c" = "b"–PAN (indicates the presence of PPN and $EtNO_2$); "d" = $EtNO_2$ reference spectrum.

It is clear that ethyl nitrate ($EtNO_2$—1660 and 854 cm^{-1}) is present too, and a spectrum of the pure substance is shown as the bottom trace [21].

The formation of products attributed to heterogeneous reactions was also proved. 3-Heptyl formate, which is known to be the product of the liquid phase oxidation of 2-Ethal in an oxygen atmosphere [17], was observed. A control experiment was carried out to verify that the decomposition product is 3-heptyl formate. The experiment consisted in letting oxygen flow inside a glass bubbler for 20 min through a liquid sample of 2-Ethal and collecting, at 150 K, the gases formed, to finally analyze them by IR absorption. Another control experiment was performed to determine the rate of disappearance of 2-Ethal due to heterogeneous reactions. From such rate it was possible to subtract the heterogeneous contribution to the overall kinetic process.

The main path for the photolysis of a hydrogenated aldehyde is by abstraction of the aldehydic-H by chlorine atoms, followed by reaction with O_2 to give peroxyacyl radicals (RO_2), which in the presence of high NO_2 concentrations end in the corresponding peroxyacyl nitrate:

$$RO_2 + NO_2 \rightarrow RO_2NO_2 \quad (3)$$

However, its slow decomposition regenerates NO_2 and RO_2 radicals:

$$RO_2NO_2 \rightarrow RO_2 + NO_2 \quad (3')$$

Peroxyacyl radicals undergo self-reaction or reaction with the unavoidably generated NO (resulting from the photolysis of NO_2) to form acyloxy radicals (RO), which in turn could decarboxylate yielding alkyl radicals.

Alkyl radicals follow a similar sequence of reactions to result in the formation of alkoxy radicals which have several possible reaction paths, depending on their structure (whether they are primary, secondary, tertiary, or with an OH group). Alkoxy radicals can react with NO_2 to form organic nitrates; isomerize, leading ultimately to hydroxy-aldehydes or hydroxy-ketones; react with O_2 to form aldehydes or ketones; or decompose to form products with shorter alkyl chain lengths [22].

Results obtained in previous studies for the reaction of Cl atoms with aldehydes indicate that the channel for H-abstraction at the aldehydic group accounts for 80–90% [6] of the total reaction of small aldehydes.

A tentative description of the oxidation mechanism of 2-Ethyl hexanal is given in Scheme 1. The radicals formed after the aldehydic-H abstraction (reaction 1.1 of the Scheme 1) react

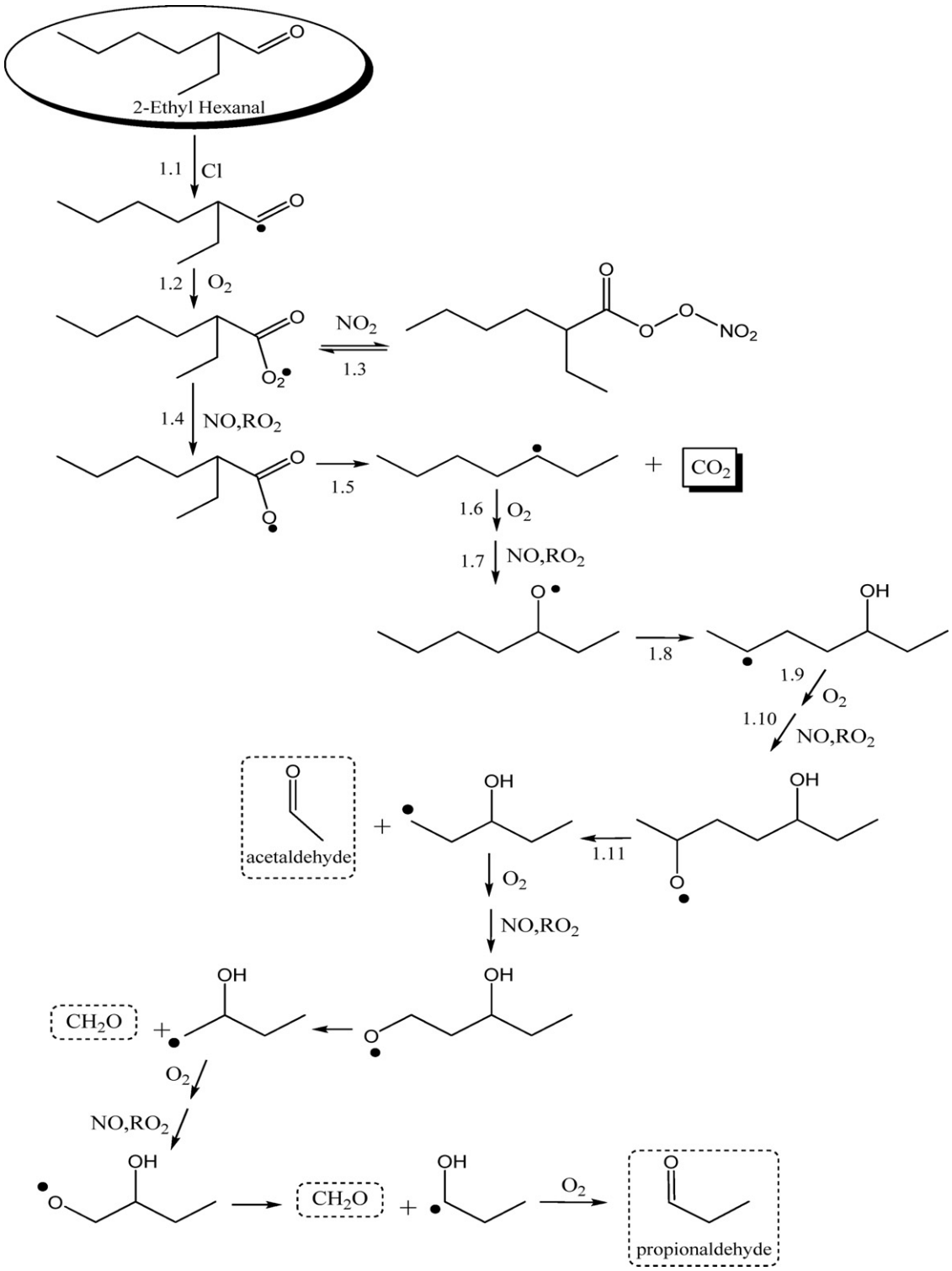

Scheme 1. Oxidation mechanism initiated by abstraction of the aldehydic hydrogen in the presence of NO_2. Products highlighted in solid boxes were identified by FTIR; formation of those in dashed rectangles was not detected, but rather deduced from the products observed and identified by FTIR.

with O_2 (reaction 1.2) to generate $C_3H_7CH_2CH(C_2H_5)C(O)O_2$ radicals ($k = 2.8 \times 10^{-12}$ cm^3 molecule^{-1} s^{-1}, assumed to be similar to $(CH_3)_2CHC(O)$) [6], which should react with NO_2 to form peroxynitrate (reaction 1.3). However, our experimental results cannot conclusively prove its presence since it was not detected by IR. The non-observation of this peroxynitrate suggests that it could be just marginally stable under our experimental conditions. To stabilize its formation, we should work at lower temperatures, but this would probably lead to an increasing contribution of the heterogeneous channel.

Reactions 1.4–1.7 are expected to be fast, as reported for related radicals [6,21], giving rise to the formation of alkoxy radicals, $C_3H_7CH_2CHO^{\bullet}$–C_2H_5, which can follow four different paths. They could react either with nitrogen dioxide or oxygen, decompose and finally, isomerize. We had no experimental indications of the first path, however (i.e. there was

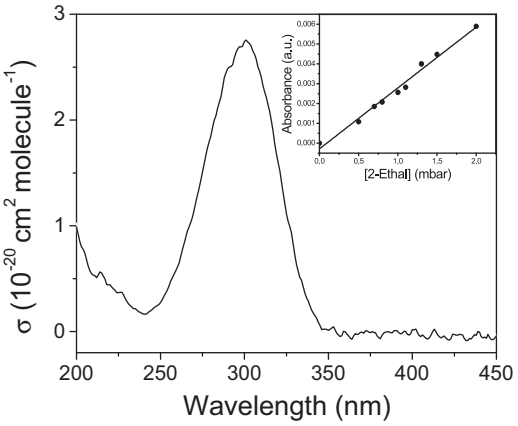

Fig. 4. UV absorption cross sections. The inset shows the calibration curve at 300 nm.

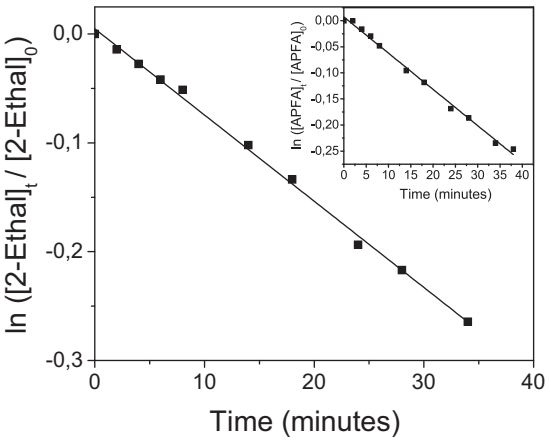

Fig. 5. Decay of 2-Ethal versus time of exposure to 254 nm radiation. The insert shows data for perfluoroacetic anhydride.

no formation of $C_3H_7CH_2C(C_2H_5)$–ONO_2); the rate of reaction with O_2 (even assumed to be similar to 2-pentoxy radical, $k = 1.2 \times 10^{-14}$ cm^3 molecule^{-1} s^{-1}) [23] would not be important; the decomposition path should also be a minor channel since the stability of this alkoxy radical is high [10]. Thus, we are left with only one channel corresponding to isomerization (reaction 1.8), which should be around 50 times faster than the three previous reactions [24].

Further reactions (i.e. with O_2 and NO, reactions 1.9 and 1.10) yield the hydroxyl-alkoxy radical for which the main path is decomposition (reaction 1.11) due to the presence of the OH group in the molecule [10]. This pathway could compete with a second isomerization, which would lead to compounds such as hydroxy-aldehydes or hydroxyl-ketones; nevertheless, no experimental evidence of these compounds has been found. Thus, the dissociation generates acetaldehyde and a shorter hydroxyl-alkoxy radical which would decompose even faster because of proximity between the OH and O in the radical. The sequence of reactions (similar to reactions 1.9–1.11) leads to formaldehyde and the next hydroxyl-alkoxy radical that finally results in formaldehyde and propionaldehyde.

A kinetic analysis of the preceding mechanism shows that aldehydes, namely formaldehyde, acetaldehyde, and propionaldehyde could be expected. Nevertheless, they were not observed since the abstraction of the aldehydic-H atom is a very fast reaction. For this reason, the aldehydes proposed have not been detected, but their oxidation products, namely PAN from acetaldehyde and PPN from propionaldehyde were detected. The abstraction reaction leads to the formation of acyl radicals, and the subsequent reaction with O_2 and NO_2 to form the peroxyacyl nitrates. In the case of formaldehyde, the radical formed leads to the elimination of CO. In the analysis of Fig. 1, PAN and PPN were detected by FTIR, as well as $EtNO_2$, coming from the decomposition of PPN.

3.3. UV absorption and quantum yield at 254 nm

The UV absorption spectrum of 2-Ethal at 298 K is shown in Fig. 4. The insert shows the linearity of the absorption with pressure. The average absorption cross sections measured are listed at 5 nm intervals in Table 2. It can be seen that 2-Ethal has a maximum UV absorption centered at around 300 nm, which is common for this type of compounds [25].

The quantum yield at 254 nm for photolysis was measured by irradiation of the gas mixtures using a low-pressure Hg lamp for as long as 30 min. Control experiments were performed to check whether the aldehyde concentration changes as a consequence of heterogeneous reactions. Thus, a mixture of 2-Ethal and oxygen was allowed into the cell in the dark and left for 30 min. After that time, a 5% decrease in the aldehyde concentration was observed. With this result, the kinetic measurements were accordingly corrected.

Fig. 5 shows a plot of the temporal variation of 2-Ethal and actinometer concentration (see insert figure). The linearity of the data shows that the two decays follow first-order kinetics. Loss rates of $(6.35 \pm 0.09) \times 10^{-5}$ s^{-1} and $(3.16 \pm 0.05) \times 10^{-3}$ s^{-1}, respectively, were determined. The errors reported correspond to a standard deviation for the actinometer, whereas for 2-Ethal errors also include the correction factor that takes into account the heterogeneous contribution.

The quantum yield presented in Table 3 was derived from equation:

$$\frac{k_{\text{2-Ethal}}}{k_{\text{actinometer}}} = \frac{\sigma_{254\,\text{nm 2-Ethal}} \times \phi_{254\,\text{nm 2-Ethal}}}{\sigma_{254\,\text{nm actinometer}} \times \phi_{254\,\text{nm actinometer}}}$$

The value for $\sigma_{254\,\text{nm 2-Ethal}}$ measured in this work (Table 2), together with literature data for $\sigma_{254\,\text{nm actinometer}}$ and $\phi_{254\,\text{nm actinometer}}$ [26] were used (see Section 2.2.3). The table also presents quantum yield values for other aldehydes. It can be seen that values for linear chain aldehydes with three to nine carbon atoms range from 0.25 to 0.30, which is about the double for the corresponding values of α-branched aldehydes. The yield of 2-Ethal is consistent with those expected for branched aldehydes, and therefore, it almost doubles the yield of n-hexanal [27].

3.4. Photolysis mechanism in the presence of O_2

Fig. 6 shows the IR features of the products of a typical photolysis experiment. CO (2235 and 2037 cm^{-1}), 3-heptanone (1733 and 1358 cm^{-1}), 3-heptanol (3660 cm^{-1}), n-heptane (1384 cm^{-1}), and CO_2 (2384 and 2290 cm^{-1}) are formed, the latter probably as a consequence of heterogeneous reactions. Its presence agrees with the results obtained by Tadić et al. in the photolysis of n-hexanal/O_2 mixtures [13]. The other products could be explained turning to Scheme 2, which shows the proposed mechanism where two primary paths can be distinguished: either a molecular mechanism resulting in unsaturated molecular species (Norrish type II) and CO elimination, or a radicalary reaction (Norrish type I) leading to the fragment HCO and subsequently to CO. The products heptane, 3-heptanol and 3-heptanone were identified by FTIR. The absence of unsaturated compounds suggests that the only relevant molecular path is the CO elimination (reaction 2.3).

It is known that linear aldehydes with a chain length shorter than four carbon atoms only decompose into free radicals. In

Table 2
UV absorption cross section (10^{-20} cm^2 molecule^{-1}) of 2-Ethal at 298 K. The cross section at 254 nm is highlighted.

Wavelength (nm)	σ (error)	Wavelength (nm)	σ (error)	Wavelength	σ (error)
200	1.02 (0.07)	**254**	**0.26**(**0.04**)	305	2.72 (0.04)
205	0.75 (0.06)	255	0.43 (0.04)	310	2.37 (0.07)
210	0.55 (0.07)	260	0.60 (0.02)	315	2.10 (0.07)
215	0.64 (0.08)	265	0.90 (0.07)	320	1.61 (0.04)
220	0.38 (0.05)	270	1.14 (0.07)	325	1.12 (0.05)
225	0.33 (0.07)	275	1.49 (0.05)	330	0.73 (0.07)
230	0.28 (0.09)	280	1.90 (0.03)	335	0.40 (0.07)
235	0.21 (0.07)	285	2.11 (0.07)	340	0.23 (0.04)
240	0.16 (0.04)	290	2.50 (0.05)	345	0.04 (0.03)
245	0.20 (0.04)	295	2.64 (0.04)	350	0.01 (0.01)
250	0.21 (0.04)	300	2.73 (0.04)	355	0.02 (0.02)

contrast, linear aldehydes with a chain length longer than or equal to four carbon atoms, react by both molecular and radical channels. The individual contribution of each channel depends on the molecular structure [11]. Tadić et al. propose that the main reaction pathway for n-hexanal involves the Norrish type II reaction as the main path with a small contribution of the Norrish type I reaction [13].

Taking into account the products conclusively identified in this work, we believe that for α-branched aldehydes, only Norrish type I reaction as well as CO elimination (reactions 2.1 and 2.3) occur. The HCO radicals result in CO formation through reaction 2.2, and the alkyl radicals ($C_4H_9CH^{\bullet}C_2H_5$) react with O_2 to generate the corresponding peroxy radicals (reaction 2.5) which could recombine (reactions 2.6–2.7) leading finally to the formation of 3-heptanol and 3-heptanone. Peroxy radicals could react with HO_2 radicals (reaction 2.8) giving rise to hydroperoxy alkanes which were not observed as products. It is therefore proposed that the main pathway for the peroxy radicals is recombination. The unavoidable

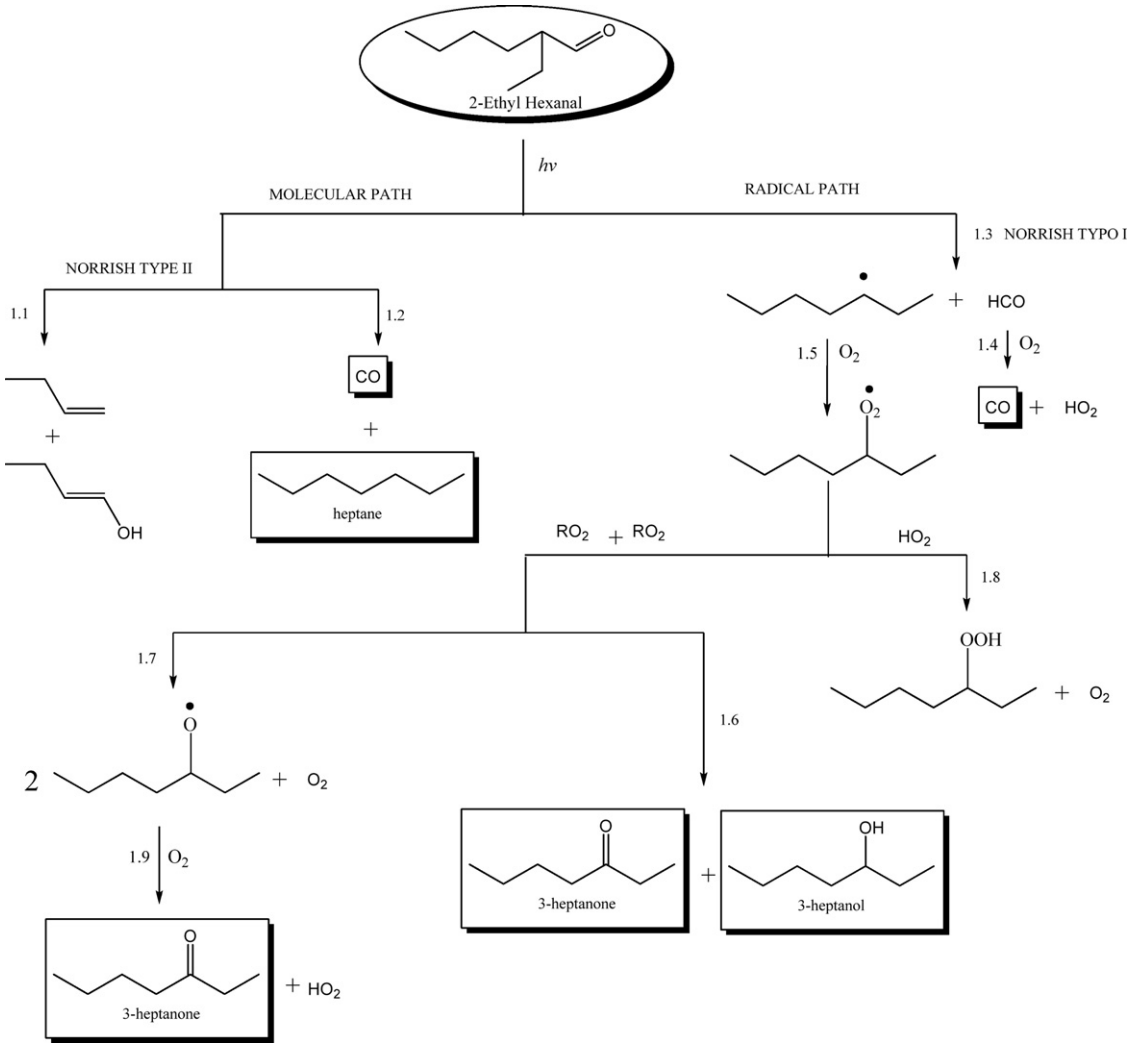

Scheme 2. Photo-oxidation mechanism of 2-Ethal initiated by exposure to 254 nm radiation in 700 Torr of O_2. Products highlighted in boxes were identified by FTIR.

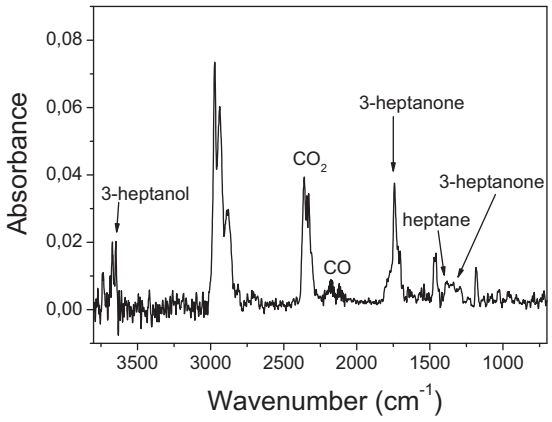

Fig. 6. Spectrum of the products of photooxidation. The formation of CO, CO_2, heptane, 3-heptanol and 3-heptanone can be observed.

Table 3
Aldehyde quantum yields at 254 nm.

Compound	$\phi_{at\ 254\,nm}$	Reference
Acetaldehyde	0.06 ± 0.05	[12,13]
Propionaldehyde	0.28 ± 0.04	
Butyraldehyde	0.20 ± 0.04	
i-Butyraldehyde	0.71 ± 0.02	
n-Pentanal	0.30 ± 0.02	
2-Methyl butyraldehyde	0.72 ± 0.03	
3-Methyl butyraldehyde	0.27 ± 0.01	
Pivaldehyde	0.56 ± 0.05	[13]
n-Hexanal	0.28 ± 0.05	
n-Nonanal	0.23 ± 0.03	
2-Ethyl hexanal	0.52 ± 0.09	This work

presence of heterogeneous processes for 2-Ethal [17] poses a limit to the quantification of the relative importance of molecular and radicalary paths.

4. Atmospheric implications

The results from the present work have important implications for the understanding of the atmospheric removal mechanism of branched-chain aldehydes.

Photolysis and oxidation are important processes in the atmospheric degradation of 2-Ethal. The relative importance of these two mechanisms is a function of altitude since the actinic flux changes with altitude, as does the OH radical concentration.

Therefore, the tropospheric removal path (mainly dominated by OH chemistry) will be different than the stratospheric one. In polluted tropospheric areas where NO_2 concentration is high, oxidation may lead to the formation of CO, CO_2, $EtNO_2$, and peroxynitrates (PAN and PPN). Peroxynitrates reaching higher altitudes, where the lower temperatures increase the residence time, could therefore be transported to unpolluted areas.

In the stratosphere, in turn, short wavelength radiation provides the main removal process through photolysis, which in the presence of O_2 may lead to the formation of alkanes (n-heptane), alcohols (3-heptanol), and ketones (3-heptanone).

Acknowledgements

Financial support from CONICET, SECYT-UNC, and FONCYT is gratefully acknowledged.

References

[1] R. Atkinson, J. Phys. Chem. Ref. Data, Monograph No. 2 (1994) 1.
[2] R. Thevenet, A. Mellouki, G. Le Bras, Int. J. Chem. Kinet. 32 (2000) 676.
[3] A. Mellouki, G. Le Bras, H. Sidebottom, Chem. Rev. 103 (2003) 5077.
[4] H. Niki, P.D. Maker, C.M. Savage, L.P. Breitenbach, J. Phys. Chem. 89 (1985) 588.
[5] F. Caralp, V. Foucher, R. Lesclaux, T.J. Wallington, M.D. Hurley, Phys. Chem. Chem. Phys. 1 (1999) 3509.
[6] J.P. Le Cráne, E. Villenave, M.D. Hurley, T.J. Wallington, S. Nishida, K. Takahashi, Y. Matsumi, J. Phys. Chem. A 108 (2004) 795.
[7] M. Manetti, F.E. Malanca, G.A. Argüello, Int. J. Chem. Kinet. 40 (2008) 831.
[8] F. Kirchner, L.P. Thüner, I. Barnes, K.H. Becker, B. Donner, F. Zabel, Environ. Sci. Technol. 31 (1997) 1801.
[9] F.E. Malanca, M. Manetti, M.S. Chiappero, P. Gallay, G.A. Argüello, J. Photochem. Photobiol. A: Chem. 205 (2009) 44.
[10] R. Atkinson, Atmos. Environ. 34 (2000) 2063.
[11] K. Wirtz, Combined US/German Environmental Chamber Workshop Riverside, 1999.
[12] G.K. Moortgat, Pure Appl. Chem. 73 (2001) 487.
[13] J. Tadić, I. Ivan Juranić, G.K. Moortgat, Molecules 6 (2001) 287.
[14] ¸C. Lehtinen, G. Brunow, Org. Proc. Res. Dev. 3 (1999) 101.
[15] R.D. Edwards, J. Jurvelin, K. Koistinen, K. Saarela, M. Jantunen, Atmos. Environ. 35 (2001) 4829.
[16] S. Nalli, O.J. Horn, A.R. Grochowalski, D.G. Cooper, J.A. Nicell, Environ. Pollut. 140 (2006) 181.
[17] M. Gliński, J. Kijeński, React. Kinet. Catal. Lett. 55 (1995) 311.
[18] M. Gliński, J. Kijeński, React. Kinet. Catal. Lett. 55 (1995) 305.
[19] R.S. Anderson, L. Huang, R. Iannone, J. Rudolph, J. Phys. Chem. A 111 (2007) 495.
[20] Z.J. Li, A. Pirasteh, Int. J. Chem. Kinet. 38 (2006) 386.
[21] R. Atkinson, D.L. Baulch, R.A. Cox, J.N. Crowley, R.F. Hampson, R.G. Hynes, M.E. Jenkin, M.J. Rossi, J. Troe, T.J. Wallington, Atmos. Chem. Phys. 4 (2004) 1461.
[22] J.J. Orlando, G.S. Tyndall, T.J. Wallington, Chem. Rev. 103 (2003) 4657.
[23] N. Meunier, J.F. Doussin, E. Chevallier, R. Durand-Jolibois, B. Picquet-Varrault, P. Carlier, Phys. Chem. Chem. Phys. 5 (2003) 4834.
[24] R. Mereau, M.T. Rayez, F. Caralp, J.C. Rayez, Phys. Chem. Chem. Phys. 5 (2003) 4828.
[25] L. Zhu, Y. Tang, J. Phys. Chem. A 108 (2004) 8307.
[26] M.S. Chiappero, F.E. Malanca, G.A. Argüello, S.T. Wooldridge, M.D. Hurley, J.C. Ball, T.J. Wallington, R.L. Waterland, R.C. Buck, J. Phys. Chem. A 110 (2006) 11944.
[27] C.A. Cuevas, A. Notario, E. Martinez, J. Albaladejo, Atmos. Environ. 40 (2006) 3845.